Computer based comparison analysis of single and double–connecting–rod slider–crank linkages

A. Aan and M. Heinloo

Institute of Technology, Estonian University of Life Sciences, Kreutzwaldi 56, EE51014 Tartu, Estonia; e-mail: aare.aan@emu.ee

Abstract. This paper presents the results of comparative numerical analysis of single and double–connecting–rod slider–crank linkages on the worksheet of Computer Package Mathcad. On the base of composed virtual models of both linkages the motion of the slider (piston) in these linkages is studied thoroughly. This paper has the links to the video clips, comparing the motions of single and double–connecting–rod slider–crank linkages and visualizing the change of vectors of velocities and accelerations in the pivot, where connects two links of double connecting rod. Concluded, that the motion of the slider (piston) and the force of reaction to the track of slider (wall of a cylinder) in these linkages is quite different.

Key words: machine and mechanism theory, linkages, internal combustion engines.

Introduction

Slider–crank linkages can be used in pumps, compressors, internal combustion engines etc. A typical scheme of one cylinder of a four-stroke internal-combustion engine with single connecting rod crank-slider linkage is shown in Fig. 1 (Merriam-Webster, 2006).

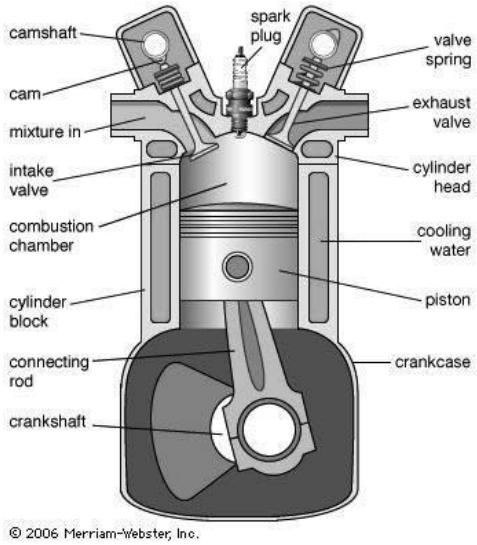

Fig. 1. Cross section showing one cylinder of a four-stroke internal-combustion engine.

A review of different internal combustion engines using single–connecting–rod crank–slider mechanism with multiple cylinders is given in Automotive Handbook (1996).

Mederer (Evert, 2003) proposed to use a double–connecting–rod linkage (Fig. 2) in combustion engines.

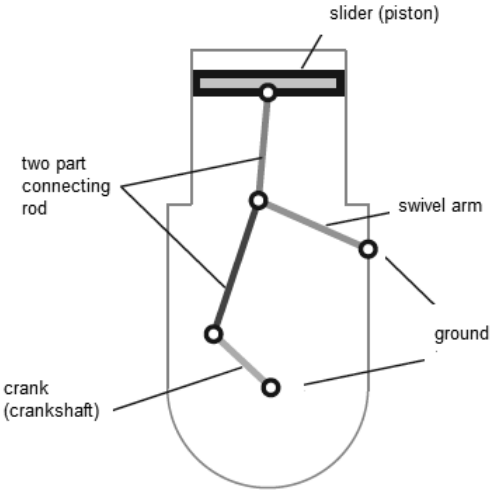

Fig. 2. The scheme of a double–connecting–rod linkage, proposed by Mederer to use in internal combustion engines.

Double–connecting–rod linkage (Fig. 2) consists of ground (cylinder), crank (on crankshaft), two part connecting rod, slider (piston) and a swivel arm. By Mederer this mechanism reduces consumption of fuel and lower emissions, because piston will stay relative long times at area of its uppermost position, and in the compression stroke large parts of counter-pressure is taken by swivel arm, that means less input power is needed for turning a crank in the compression stroke.

The aim of this paper is to present the method and results of comparative numerical analysis of single–connecting–rod and double–connecting–rod slider–crank linkages on the worksheet of Computer Package Mathcad, in the case of constant (idle) crank (crankshaft) angular velocity. On the base of composed virtual models of both linkages the motion of the slider (piston) in these linkages will be studied thoroughly. This paper will have also links to two composed video clips. First video clip compares the motions of single–connecting–rod and double–connecting–rod slider–crank linkages with the same maximum displacement of the slider (piston). Second video clip visualizes the changing geometrical vectors of velocities and accelerations in the pivot, where connects two links of double-connecting-rod slider–crank linkage. This video clip compares also the reaction force in the track of sliders (cylinder wall).

Composition of virtual models of linkages

The links OA, AE, and EC of the four-bar OAEC in the structure of double–connecting–rod linkage can rotate around pivots O, A, E and C, whereby pivots O and C are grounded (Fig. 3). For numerical computations let us assume that the lengths of

the links OA, AE and EC are l_{OA} = 0.3 m, l_{AE} = 0.7 m, l_{EC} = 0.735 m accordingly and the coordinates of the pivot C are x_C = 0.67 m, y_C = 0.7 m. Let us suppose also that the rotational speed of crank OA is n = 700 rpm, that means angular velocity ω = 73.304 rad s^{-1}.

The coordinates of pivot A (Fig. 3) can be found out by equations

$$x_A(\varphi) = l_{OA} \cdot \sin\varphi, \qquad y_A(\varphi) = l_{OA} \cdot \cos\varphi.$$

The four-bar OAEC has constraints that the distances between pivots A, E and E, C are permanent. Mathematically these constrains means the following system of nonlinear equations of constraints

$$\begin{aligned} (x_E - x_C)^2 + (y_E - y_C)^2 &= {l_{EC}}^2, \\ (x_E - x_A(\varphi))^2 + (y_E - y_A(\varphi))^2 &= {l_{AE}}^2, \end{aligned} \tag{1}$$

where φ is the angle of rotation of the crank OA from y-axis clockwise.

The system of equations (1) was solved on the worksheet of Mathcad numerically relative to x_E and y_E (Fig. 3).

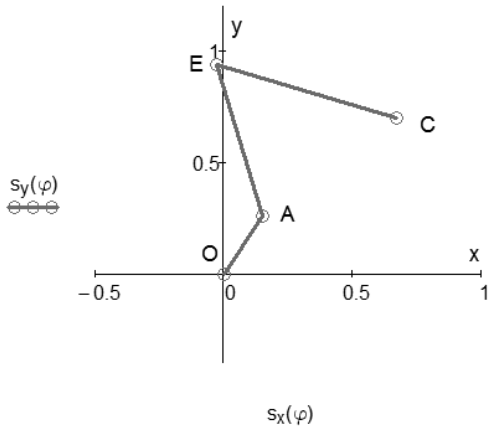

Fig. 3. The virtual model of four-bar OAEC under crank's rotation angle φ=30°.

Let us compose the following column vectors

$$s_x(\varphi) = \begin{pmatrix} 0m \\ x_A(\varphi) \\ x_E(\varphi) \\ x_C \end{pmatrix}, \qquad s_y(\varphi) = \begin{pmatrix} 0m \\ y_A(\varphi) \\ y_E(\varphi) \\ y_C \end{pmatrix}.$$

Fig. 3 shows the virtual model of linkage OAEC, drawn by these vectors on the worksheet of Mathcad.

Connecting to the pivot E of four-bar in Fig. 3 by a link ED to the pivot pivot D, what is moving along y-axis, we get a virtual model of double-connecting-rod linkage on Figs 2 and 4. Let the length of the link ED be l_{ED} = 0.7 m. The y-coordinate of pivot D can be find out from the following equation of restriction

$$y_D(\varphi) = y_E(\varphi) + \sqrt{{l_{ED}}^2 - x_E(\varphi)^2}. \quad (2)$$

The following vectors

$$s'_x(\varphi) = \begin{pmatrix} x_E(\varphi) \\ 0 \end{pmatrix},$$
$$s'_y(\varphi) = \begin{pmatrix} y_E(\varphi) \\ y_D(\varphi) \end{pmatrix},$$

draw on the worksheet of Mathcad the virtual model of double–connecting–rod crank–slider linkage in Fig. 4a.

To compose the virtual model for typical single–connecting–rod crank-slider linkage in Fig. 4b, we used the following equation of constraint

$$l'_{AD} = \sqrt{(y'_D(\varphi) - y_A(\varphi))^2 + x_A(\varphi)^2}, \quad (3)$$

where l'_{AD} is the permanent length of the link AD in Fig. 4b. In computations were taken $l'_{AD} = l_{AE} + l_{ED} = 1.4$ m. Equation (3) determine the coordinate $y'_D(\varphi)$ of the pivot D by the following formula

$$y'_D(\varphi) = y_A(\varphi) + \sqrt{{l_{AD}}^2 - x_A(\varphi)^2}.$$

The following vectors

$$ss_x(\varphi) = \begin{pmatrix} 0m \\ x_A(\varphi) \end{pmatrix},$$
$$ss_y(\varphi) = \begin{pmatrix} 0m \\ y_A(\varphi) \end{pmatrix},$$
$$ss'_y(\varphi) = \begin{pmatrix} y'_D(\varphi) \\ y_A(\varphi) \end{pmatrix},$$

draw on the worksheet of Mathcad the virtual model of single–connecting–rod crank–slider linkage in Fig. 4b.

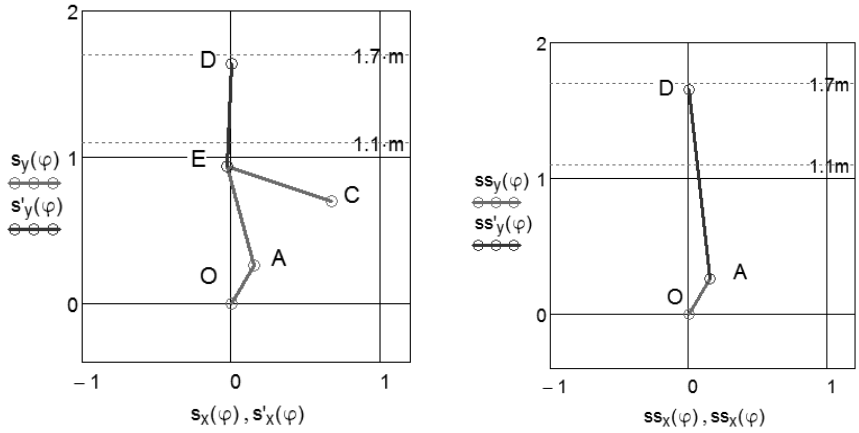

Fig. 4. The virtual models of double–connecting–rod (a) and single–connecting–rod (b) crank–slider linkages under crank's rotation angle $\varphi = 30°$.

Comparison of displacement, velocity and acceleration of a slider (piston)

To compare of displacement, velocity and acceleration, let´s give for rotation angle φ the values from 0 with step 0.1 up to $4 \cdot \pi$. This means that the crank OA in Fig. 4 makes two rotations.

According to used assumption, in Fig. 5 at the bottom dead centre (BDC) and the top dead centre (TDC) the pivot D (slider) virtual model displacements for both cases (Fig. 4a and Fig. 4b) are coincidence, but between BDC and TDC displacements are different.

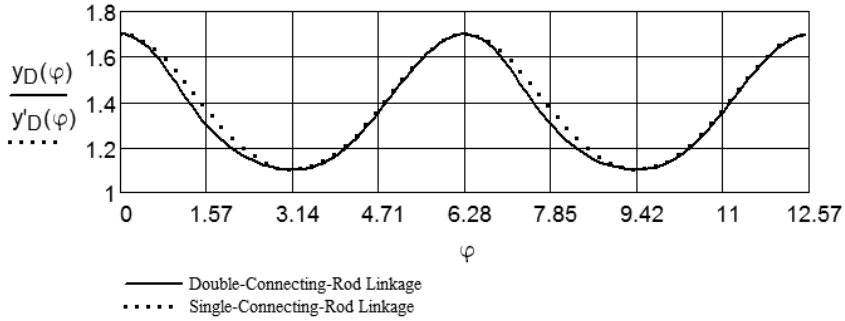

Fig. 5. The Displacement of pivot D (slider) for double–connecting–rod and single–connecting–rod crank–slider linkages dependence from rotational angle φ.

The velocity projections of pivot's D (Fig. 4) are

$$v_{Dy}(\varphi) = \frac{d}{d\varphi} y_D(\varphi) \cdot \omega, \quad v'_{Dy}(\varphi) = \frac{d}{d\varphi} y'_D(\varphi) \cdot \omega.$$

Fig. 6 shows the change of projections of the velocity of the pivot D (Fig. 4) for both virtual models. One can conclude in range of TDC these projections are coincident for both virtual models, but in BTC are not.

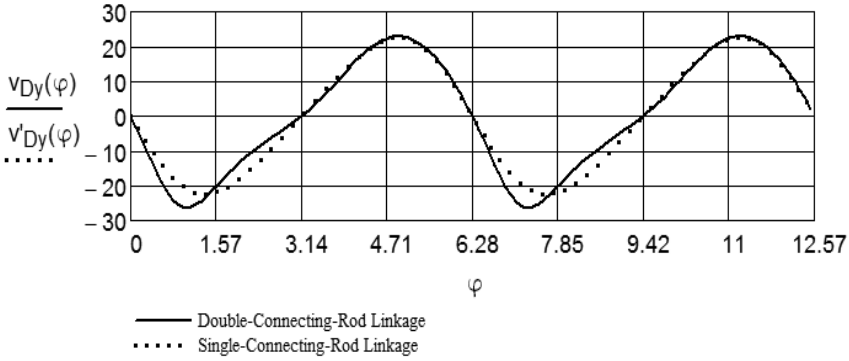

Fig. 6. The velocity of pivot D (slider) for double–connecting–rod and single–connecting–rod crank–slider linkages dependence from rotational angle φ.

The accelerations projections of pivot's D (Fig. 4) are

$$a_{Dy}(\varphi) = \frac{d^2}{d\varphi^2} y_D(\varphi) \cdot \omega^2, \qquad a'_{Dy}(\varphi) = \frac{d^2}{d\varphi^2} y'_D(\varphi) \cdot \omega^2.$$

One can conclude from Fig. 7 shows that the projections of accelerations of the pivot D for both virtual models are quite different.

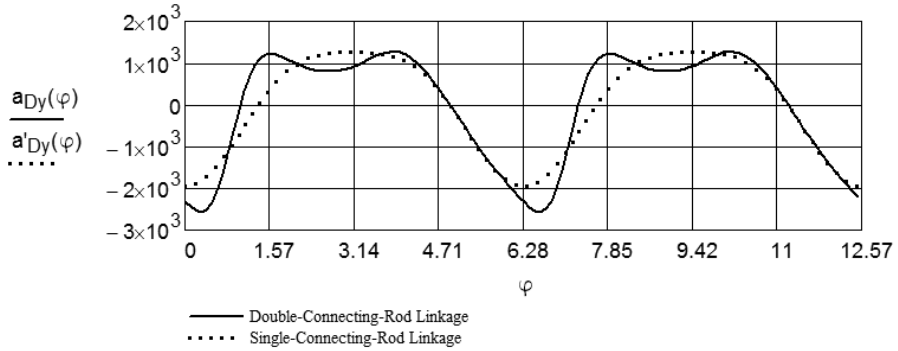

Fig. 7. The accelerations of pivot D (slider) for double–connecting–rod and single–connecting–rod crank–slider linkages dependence from rotational angle φ.

Comparison of angles between the link, connected to the pivot of the slider (piston) and the track of motion

Angles between y-axis (pivot D track) and the links on single connecting rod AD and double connecting rod ED (pressure angle (Kleis, 1988), can be found out from the equations

$$\beta(\varphi) = asin\frac{x_E(\varphi)}{l_{ED}}, \qquad \beta'(\varphi) = asin\frac{x_A(\varphi)}{l_{AD}}.$$

Fig. 8 shows that the pressure angle β for double–connecting–rod linkage is lower than the correspondent angle β' for single–connecting–rod linkage.

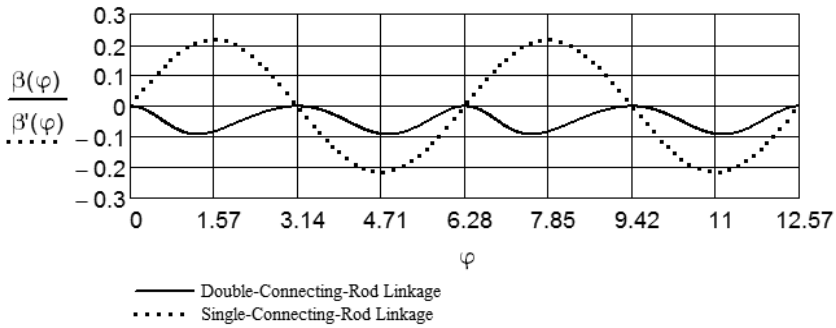

Fig. 8. The pressure angle between the links ED and AD (Fig. 4) relative to the y-axis (track of pivot D) for double–connecting–rod and single–connecting–rod crank–slider linkages dependence from rotational angle φ.

Comparison of the reaction force from the track of slider (the wall of cylinder)

Let´s apply force F_D = 1000 N to the slider pivot (piston) and take the mass of slider (piston) equal to m_k = 3 kg. The equations of motion of the slider (piston) are

$$m_k \cdot a_{Dy}(\varphi) = -F_D + R_E(\varphi) \cdot \cos\beta(\varphi),\ 0 = R_{Dx}(\varphi) + R_E(\varphi) \cdot \sin\beta(\varphi), \quad (4)$$

where $R_E(\varphi)$ – is the reaction force, applied from link ED in Fig. 4 (a) to the pivot D, $R_{Dx}(\varphi)$ – is the projection of the reaction force, applied to the track of slider (cylinder wall).

From equations (4) one can get the following formula for determination the projection of the reaction force $R_{Dx}(\varphi)$

$$R_{Dx}(\varphi) = (m_k \cdot a_{Dy}(\varphi) + F_D) \cdot \tan\beta(\varphi).$$

Analoguous formula is valid for the case Fig. 4b

$$R'_{Dx}(\varphi) = (m_k \cdot a'_{Dy}(\varphi) + F_D) \cdot \tan\beta'(\varphi).$$

From Fig. 9 follows that the average reaction force in the case double–connecting–rod linkage is lower than in the case of single–connecting–rod linkage that means less friction between slider and track (piston and cylinder wall) in double–connecting–rod linkage.

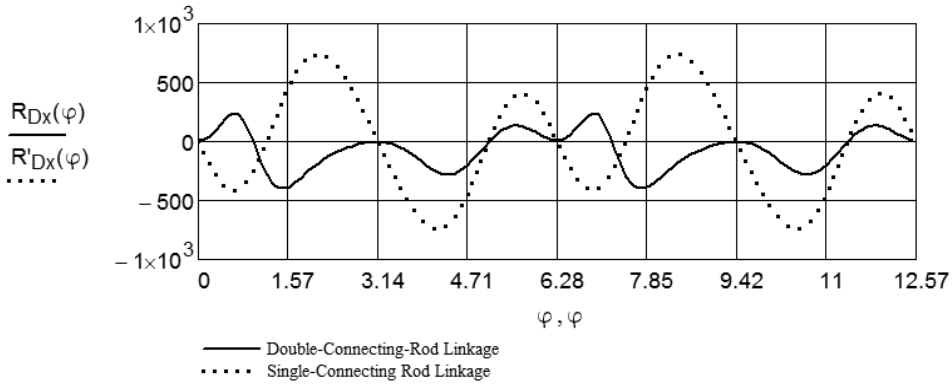

Fig. 9. The projections of the reaction forces between the slider and its track (piston and cylinder) for double–connecting–rod and single–connecting–rod crank–slider linkages dependence from rotational angle φ.

Comparison of visualizing video clips

The Computer Package Mathcad allows also compose of video clips. To visualize the obtained solution and to verify it, two video clips were made. The video clip (Aan & Heinloo, 2012-1), composed on the base of Figs 4 and 5, show visually the change of co-ordinate of pivot D in accordance with motion of corresponding linkage. The video clip (Aan & Heinloo, 2012-2), composed on the base of Figs 4 and 9, shows visually the dependence of reaction force between the link D and the track of it (piston and cylinder wall) in accordance with motion of corresponding linkage. Also on that video clip is visualized change of geometrical vectors of velocity and acceleration of the pivot D and pivot E. These vectors were composed by using the special program on the worksheet of Mathcad, presented by Bertjajev (2005).

Conclusions

- The motion of the slider (piston) in double-connecting-rod linkage and single–connecting–rod linkage is quite different.
- The slider (piston) of double-connecting-rod linkage has lower reaction force on the track of motion (cylinder wall). That means the force, applied to the slider (piston) in double–connecting–rod linkage makes more useful work. Therefore, the motor based on double–connecting–rod linkage could have lower consumption of fuel and lower emissions than the motor with single–connecting–rod linkage.
- The Computer Package Mathcad can be used as convenient tool for composition of video clips for visualization and verify the obtained solution.
- The method and the results of study may be used by teachers of engineering subject ‘Machine and Mechanism Theory’ and by automobile engineers.

References

Merriam-Webster. 2006. Internal combustion engine. Available at: http://www.merriam-webster.com/concise-images/72180.htm (02.02.2012).

Robert Bosch GmbH. 1996. *Automotive Handbook 4th edition*. Stuttgart, pp. 892.

Evert, A. 2003. Buckle- and Double-Connecting-Rod. Available at: http://www.evert.de/eft774e.htm (02.02.2012).

Kleis, I. 1988. *Applied mechanics*. Valgus. Tallinn, pp. 423. (in Estonian).

Aan, A., Heinloo, M. 2012. Comparison of piston displacements. Available at: http://youtu.be/LG2h8oiyjIU (02.02.2012).

Aan, A., Heinloo, M. 2012. Comparison of piston velocities accelerations and reactions. Available at: http://youtu.be/QvyZAo-Q3Rk (02.02.2012).

Bertjaev, B. D. 2005. *Mathcad–based Training in Theoretical Mechanics.* Sankt-Peterburg, pp. 738. (in Russian).